People's Democratic Republic of Algeria
Ministry of Higher Education and Scientific research
M'hamed Bougara University, Boumerdes
Institute of Electrical and Electronic Engineering,
Laboratory of Signals and Systems (LSS)

ALGERIAN JOURNAL OF SIGNALS AND SYSTEMS

ISSN : 2543-3792

Title: **Induction Motor Faults Detection Using a Statistical Procedure Based-Approach**

Authors: **A. Kouadri, A. Kheldoun, M. Hamadache, L. Refoufi**

Affiliations:
Signals and Systems Laboratory, IGEE, UMBB University, 35000; Boumerdes, Algeria,

Page range: **130- 139**

Volume : 2 Issue : 3 (September 2017)

Laboratory of Signals and Systems
Address : IGEE (Ex-INELEC), Boumerdes University, Avenue de l'indépendance, 35000, Boumerdes, Algeria
Phone/Fax : 024 79 57 66
Email : lss@univ-boumerdes.dz ; ajsyssig@gmail.com

Induction Motor Faults Detection Using a Statistical Procedure Based-Approach

Kouadri A., Kheldoun A., Hamadache M., Refoufi L.
Signals and Systems Laboratory, Institute of Electrical and Electronic Engineering
University of Boumerdes, Avenue of the Independence, 35000, Boumerdès, Algeria.
Email: ab_kouadri@hotmail.com, aissakheldoun@gmail.com

Abstract: This paper presents the application of a new technique based on the variance of three phase stator currents' instantaneous variance (VIV-TPSC) to detect faults in induction motors. The proposed fault detection algorithm is based on computation of the confidence interval index (CI) at different load conditions. This index provides an estimate of the amount of error in the considered data and determines the accuracy of the computed statistical estimates. The algorithm offers the advantage of being able to detect faults, particularly broken rotor bars, independently of loading conditions. Moreover, the implementation of the algorithm requires only the calculation of the variance of the measured three-phase stator currents' instantaneous variance. The discrimination between faulty and healthy operations is based on the adherence of VIV-TPSC value to the CI which is calculated after checking out that the variance of instantaneous variance is a random variable obeying to normal distribution law. Rotor and stator resistance values are not used in any part of the CI and VIV-TPSC calculations, giving the algorithm more robustness. The effectiveness and the accuracy of the proposed approach are shown under different faulty operations.

Keywords: Induction motor; fault detection; variance of three phase stator currents' instantaneous variance; Confidence Interval.

1. INTRODUCTION

Despite the fast development and technological advances in the control and automation of complex processes, monitoring is a very important task which still remains largely a manual activity, carried out by operators, especially when it comes to respond to abnormal faulty operations; particularly in relation to induction motors, a center piece of motion power in industrial processes. Therefore, the diagnosis and repair of faults are of great importance to prevent costly damages and downtimes. Investigations on different failure modes in induction motors have revealed that up to 10% of the overall motor faults are related to cracked or broken rotor bars [1]. Operation of IM with broken rotor bars may not only damage the motor itself, but also have a very negative impact on the other system components.

Many types of fault detection techniques have been developed but the main type of techniques are based on using the stator current to sense rotor faults as well as stator faults [2]–[10]. Each fault type is recognized by appropriate harmonic spectra. The harmonics in the stator current produced by rotor eccentricity are different from those produced by broken bars and those produced by bearings failure too [11]-[14]. All these harmonics must be separated from the fundamental one, requiring adequate skills to perform accurate analyses. Using different wavelet schemes have proven effective [15]-[20]. In [15], it suggested to apply DWT to the reactive power signal in order to detect broken rotor bars in induction motors under transient load conditions. Frequency analysis of the last four obtained approximations and details components at decomposition level 12 using mother wavelet Daubechies 5 are only used. The oscillations on these signals indicate the fault occurrence and the number of broken rotor bars. Furthermore, a defined faulty severity factor (FSF) is evaluated and by which the motor conditions regarding the broken rotor bars fault are classified. However, besides the load sensitivity (greater than 20% of rated load), DWT decomposition level cannot be generalized as well as FSF. In [16], a DWT –based approach is used for IM broken rotor bars diagnosis taking the type of power supply into account (direct line or inverter). The method is based on the computation of a variability factor to be compared with pre-established thresholds for decision making on the motor condition. The technique cannot be easily generalized for other induction motor sizes besides that the DWT decomposition level is not the same for the same types of faults [15]- [20].

Condition monitoring for different types of rotating machine faults detection and localization using

mechanical sensors, primarily vibration sensors based on proximity probes can be used as in [21]. However, these approaches are delicate and expensive [22].

Model-based diagnosis methods consider a structural model of the behavior of the process based on fundamental physical principles. In [23], a model has been developed showing the relationship between faults which lead to asymmetry in the machine impedance and the consequence that is the unbalanced phase currents. Therefore by measuring the negative-sequence currents flowing in the line, the fault can be detected [24, 25]. However, negative-sequence currents can also be caused by voltage unbalance, machine saturation, etc, besides its sensitivity to slip and temperature variation. A Power Decomposition Technique (DPT) has been used in [26] to decrease sensitivity and harmonics effects; however, the detection procedure becomes cumbersome for implementation in industrial environment.
Statistical-based IM broken rotor bars faults detection methods have been investigated in [27] and [28]. In [27], a fault index ratio is proposed to discriminate between one, two, or three broken rotor bars faults independently of motor load conditions. The fault index is the ratio of standard deviation to mean absolute value of stator current. However, this approach cannot hold if voltage unbalance fault is considered. As the mean absolute value is affected hence jeopardizing the faults discrimination process. A multi-combined faults detection method is implemented using FPGA board in [28]. The method uses a feedforward Artificial Neural Network (ANN) whose parameters (weights and biases) are obtained offline. The training data are the information entropy, the mean and the variance which are obtained from measuring the steady-state stator current for different considered faults (voltage unbalance, bearing's outer race damage and broken rotor bar). This approach has been applied to a 1-hp induction motor and cannot be easily generalized to other IM sizes, except at the cost of a large training data needed to train the ANN.
In this work it is proposed the use of the variance of three-phase stator currents' instantaneous variance in detecting faults in induction motors. The detection algorithm has the important advantages of being simple, load-insensitive and based on the computation of only one parameter, the confidence interval index (CI). The index provides an estimate of the amount of error in the considered data and characterizes the accuracy of the computed statistical estimates. The data variability may result from random measurement errors caused by the system parameters uncertainties, internal and external noises, and also measuring instruments inaccuracies.

2. EXPERIMENTALSETUP

A low-voltage induction motor test facility was installed. It allowed the testing of a direct-on-line 3-phase squirrel cage induction motor which could be quickly and easily replaced as necessary, under repeatable and wholly realistic operating conditions. The mounted induction motor is directly coupled with a loading DC generator. The rotor of the DC generator is connected to an electrical loading bank so that the electrical energy generated could be dissipated as heat. The load could be set at 0%, 25%, 50%, 75% or 100% of the maximum rated load - based on the output torque – by switching-in different resistor combinations within the electrical loading bank whilst the rig was online. Two different test motors have been used in the present work.

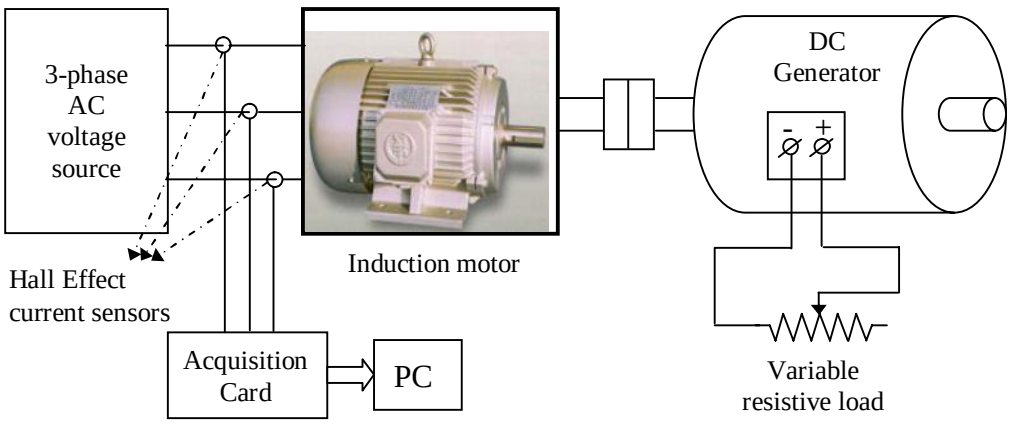

Figure 1: Schematic of the experimental set-up

The 3kW squirrel cage induction motor whose parameters are given in the first row of table 1, has been used for the broken rotor bars test. The second motor which has the parameters shown in the second row of table 1 has been used for the voltage unbalance test.

Table 1: Test motors' specifications

		Motor	
		#1	#2
Parameters	Number of poles	4	4
	Stator winding connection	Y	Y
	Rated voltage	380 V	380 V
	Rated current	8 A	5 A
	Rated power	3 kw	2.2 kw
	Rated speed	1410 r.p.m	1430 r.p.m
	Number of stator slots	36	36
	Number of rotor bars	28	32

3. PROPOSED FAULT DETECTION SCHEME

In practice, the signal variability may result only from random measurement errors. Instrument measurements are often not perfectly accurate. It can be assumed that the quantity being measured is stable and that the variation between measurements is caused by observational errors. For current measurements, Hall Effect current sensors are used.

These measurements are usually affected by random noise that is inherently due to the physical limitations of measuring instruments in terms of response time, and actuators reaction time. In addition, the dynamics are often overlooked as a source of significant errors causing extensive parametric variations in the overall process. The friction constants and geometric parameters are usually uncertain and may change during the operating process. For these reasons, it becomes worth investigating the benefits of the use of a specific technique based on the variance of the three instantaneous stator currents' instantaneous variance in view of achieving a better fault detection capability in an induction motor systems.

The instantaneous variance can constitute an adequate tool for measuring the degree of randomness of a given effect. It changes from one sample time to another under healthy conditions; therefore it can be classified as a random variable representing the effect under study. For each sample time an instantaneous variance $\sigma_i^2, i = 1,\ldots,N$, is calculated as shown in equation 1.

$$\sigma_i^2 = \frac{1}{3}\sum_{j=1}^{3}\left(i_{i,j} - m_i\right)^2 \quad (1)$$

where $i_{i,j}$ defines the current of phase *j* at sampling time *i* and m_i that represents the instantaneous mean of the three stator currents is given as follow

$$m_i = \frac{1}{3}\sum_{j=1}^{3} i_{i,j} \quad (2)$$

For a given time window, the variance of instantaneous variance σ_x^2, being as a fault detection index, is computed where *x* represents the instantaneous variance set of the three stator currents. The obtained sequence $\left\{\sigma_{x,1}^2, \sigma_{x,2}^2, \ldots, \sigma_{x,N}^2\right\}$ defines a random variable Σ of a mean $m_{\sigma_x^2}$ and a variance $\sigma_{\sigma_x^2}^2$.

In a practical situation, the proposed fault detection approach is based on two principles; (*a*) the collection of current data sets under the healthy mode of operating and at different loads with

statistical analysis of the signals, (*b*) testing according to statistical characteristics established in part (*a*) under faulty mode.

For the purpose of fault detection, it is required to evaluate the Confidence Interval for the random variable Σ. A fault is detected if the variance of the three phase currents' instantaneous variance does not belong to the established confidence interval. To increase the sensitivity of the fault detection index, a confidence interval containing a given mean σ_x^2 with an acceptable probability should be a priori set up. This probability defines a confidence level $(1-\alpha)$ which is typically fixed at 95%.

For normally distributed data, we define the confidence interval, known as the $(1-\alpha)$x100% confidence interval where α represents the error risk incurred by assert that σ_x^2 is located in the considered interval. The confidence interval ($CI_{\sigma_x^2}^{1-\alpha}$) proposes an estimate of the amount of error involved in the considered data and characterizes the precision of the computed statistical estimates.

For a relatively large number of experiments ($N \geq 50$), the law of the shifted and scaled random variable can be approximated by the normal distribution law *N*(0,1). The $(1-\alpha)$x100% confidence interval of a random variable Σ at an error risk level α is given by:

$$CI_{\sigma_x^2}^{1-\alpha} = \left] m_{\sigma^2_{\sigma_x^2}} - 1.65\sigma_{\sigma^2_{\sigma_x^2}}, m_{\sigma^2_{\sigma_x^2}} + 1.65\sigma_{\sigma^2_{\sigma_x^2}} \right[\quad (3)$$

The probabilistic computing of the fault detection index estimate, based on the variance of three-phase stator currents' instantaneous variance, and its corresponding $(1-\alpha)$x100% confidence interval (3) are based on the fact that the random variable Σ approximately follows a normal distribution law of with mean $m_{\sigma^2_{\sigma_x^2}}$ and standard deviation $\sigma_{\sigma^2_{\sigma_x^2}}$. However, an appropriate statistical test is required to examine the validity of the results, which can be accomplished using the Kolmogorov-Smirnov test [29]. This choice is closely linked to the measures, distribution frequencies of the random variable Σ, and number of available samples. Specifically, Kolmogorov-Smirnov test creates in a given sample, a vector of cumulative frequency of the random variable Σ obeying a normal distribution law *N*($m_{\sigma^2_{\sigma_x^2}}$, $\sigma_{\sigma^2_{\sigma_x^2}}$). The cumulative frequencies which represent the distribution function are obtained from the probabilities p_k assessed for any $\sigma^2_{\sigma_x^2}$ less than σ^2 and are given by:

$$F_k = \sum_{\sigma^2_{\sigma_x^2,k} < \sigma^2} p_k \quad (4)$$

Thus, an empirical integral law F of a mean $m_{\sigma^2_{\sigma_x^2}}$ and a standard deviation $\sigma_{\sigma^2_{\sigma_x^2}}$ is defined in order to satisfy, for all $\sigma^2 \in \Re$, the condition $|F_k - F| \to 0$ and consequently:

$$\sup_{\sigma^2 \in \Re} |F_k - F| \to 0 \quad (5)$$

This means the largest difference between F_k and F tends to zero in probability.

The non-parametric Kolmogorov-Smirnov test of the variance of three-phase stator currents' instantaneous variance (VIV-TPSC) is used in validating that the random variable Σ is normally distributed. The effectiveness and accuracy of the proposed fault detection index in detecting faults is tested by its adherence to the corresponding $(1-\alpha)$x100% confidence interval.

4. ANALYSIS OF THE EXPERIMENTAL RESULTS

The variance of the three phase currents' instantaneous variance is calculated from three independent runs of the induction motor which operates under healthy mode. The three runs correspond to 0%, 50% and full load operation respectively. Each run consists of 73 repeated 7 and double periods' parts for motor #1 and motor #2, respectively. Where, one period represents 65 samples. This number of periods covers all harmonics which can appear in the presence of any fault in the induction motor. In addition, it is chosen in order that VIV-TPSC is normally distributed. However, it is fixed for different used statistical procedures.

At each aforementioned load and for each motor, a variance of the three phase currents' instantaneous variance is obtained. In figure 2, it is shown the frequencies appearance of the sampled VIV-TPSC under a healthy mode and at different loads. It can be seen that the sampled VIV-TPSC is relatively bell-shaped at different loads especially for the motor #2. Almost all the VIV-TPSC frequencies appearance and their corresponding estimated density function are approximately superimposed. However, from an inspection of the histogram of VIV-TPSC of the motor #1 at 0% load, it can be easily seen that the stair curve is so far the shape of a bell. In addition, the VIV-TPSC having the bell-shaped distribution is obtained by the estimated density function with mean of VIV-IPSC and standard deviation covering the most VIV-TPSC frequencies. The truth or falsity that VIV-TPSC is normally distributed at different load can be reasonably certain by using a statistical test. Indeed, in accepting the normality of VIV-TPSC at 0% load of the motor #1 is a great deal uncertain. The non-parametric Kolmogorov-Smirnov test merely implies that we have no evidence to believe by eyes the VIV-TPSC normality distribution. Therefore, the non-parametric Kolmogorov-Smirnov test is merely used to validate the normal law of the VIV-TPSC at typical error risk of 5%. The obtained *p*-values for the motor #1and motor #2, representing the probability of accepting under the assumption that the VIV-TPSC is normally distributed, are regrouped in table 2. However, the chosen error risk level is related to the degree of certainty required to reject that the VIV-TPSC sample follows a normal law. This is true if the probability of observing a sampled result is less than the error risk. Therefore, the VIV-TPSCs satisfy the normal distribution law with fairly acceptable probabilities.

In figure 3 is illustrated the 95% confidence interval for the VIV-TPSC at different loads (0%, 50% and full load) and computed for 7 and double periods for the motor #1 and motor #2, respectively. This 95% confidence interval, developed at different loads, fully satisfies the The variance of the three phase currents' instantaneous variance is calculated from three independent runs of the induction motor which operates under healthy mode. The three runs correspond to 0%, 50% and full load operation respectively. Each run consists of 73 repeated 7 and double periods' parts for motor #1 and motor #2, respectively. Where, one period represents 65 samples. This number of periods covers all harmonics which can appear in the presence of any fault in the induction motor. In addition, it is chosen in order that VIV-TPSC is normally distributed. However, it is fixed for different used statistical procedures.

Table 2: Probabilities of accepting the normality distribution of VIV-TPSC

		Load		
		0%	50%	100%
Motor	#1	0.1495	0.8453	0.1894
	#2	0.9374	0.9388	0.6044

At each aforementioned load and for each motor, a variance of the three phase currents' instantaneous variance is obtained. In figure 2, it is shown the frequencies appearance of the sampled VIV-TPSC under a healthy mode and at different loads. It can be seen that the sampled VIV-TPSC is relatively bell-shaped at different loads especially for the motor #2. Almost all the VIV-TPSC frequencies appearance and their corresponding estimated density function are approximately superimposed. However, from an inspection of the histogram of VIV-TPSC of the motor #1 at 0% load, it can be easily seen that the stair curve is so far the shape of a bell. In addition, the VIV-TPSC having the bell-shaped distribution is obtained by the estimated density function with mean of VIV-IPSC and standard deviation covering the most VIV-TPSC frequencies. The truth or falsity that VIV-TPSC is normally distributed at different load can be reasonably certain

by using a statistical test. Indeed, in accepting the normality of VIV-TPSC at 0% load of the motor #1 is a great deal uncertain. The non-parametric Kolmogorov-Smirnov test merely implies that we have no evidence to believe by eyes the VIV-TPSC normality distribution. Therefore, the non-parametric Kolmogorov-Smirnov test is merely used to validate the normal law of the VIV-TPSC at typical error risk of 5%. The obtained *p*-values for the motor #1and motor #2, representing the probability of accepting under the assumption that the VIV-TPSC is normally distributed, are regrouped in table 2. However, the chosen error risk level is related to the degree of certainty required to reject that the VIV-TPSC sample follows a normal law. This is true if the probability of observing a sampled result is less than the error risk. Therefore, the VIV-TPSCs satisfy the normal distribution law with fairly acceptable probabilities.

In figure 3 is illustrated the 95% confidence interval for the VIV-TPSC at different loads (0%, 50% and full load) and computed for 7 and double periods for the motor #1 and motor #2, respectively. This 95% confidence interval, developed at different loads, fully satisfies the condition of reliable faults and eliminates false fault detection caused by external noises and parametric variations which are significant from the dynamic standpoint of the induction motor. Consequently, it increases the fault detection index sensitivity and accuracy. The induction motor is considered to be undergoing a faulty operation, if any sampled VIV-TPSC does not belong to the corresponding confidence interval.

The 95% confidence interval calculated under the healthy mode with no and full load on the rotor shaft is considered as a threshold. Indeed, the biggest value of the CI corresponds to the healthy mode with full load operation whereas the lowest corresponds to the no-load operation. Thus, a faulty operation of the motor is detected if the measured VIV-TPSC is out the tube limited by the healthy biggest and lowest CIs.

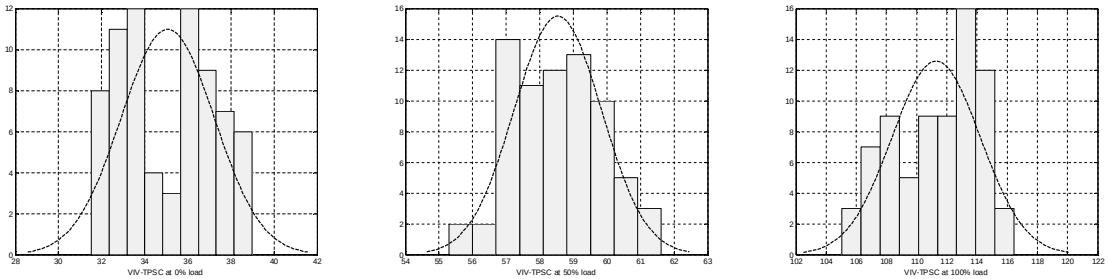

a) Motor #1

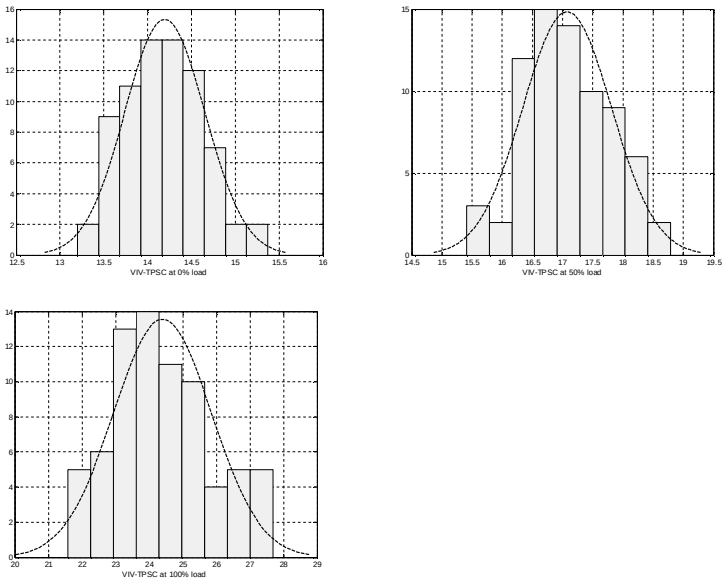

b) Motor #2

Figure 2: VIV-TPSC' histograms under healthy mode for motor #1 and motor #2 at different load conditions

To validate the proposed strategy and test the ability of VIV-TPSC in detecting various forms of faults, two types of fault operation are considered in this work: one broken bar and voltage unbalance.

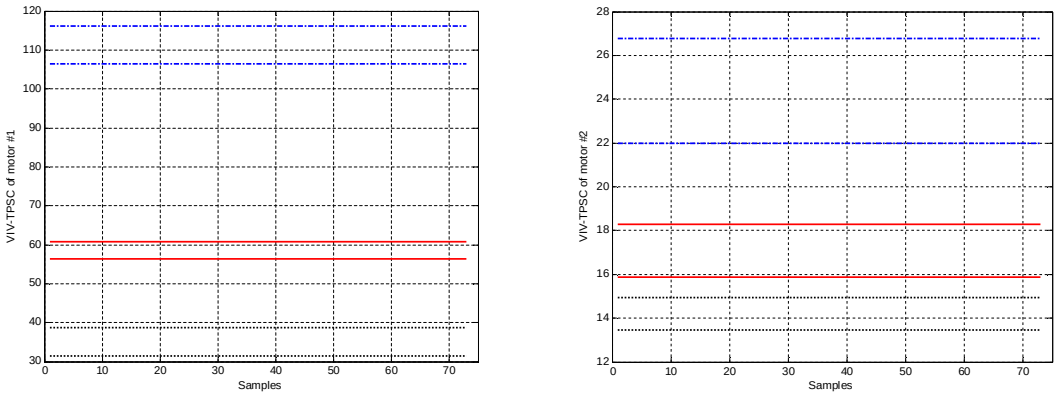

Figure 3: 95% Confidence Interval for motor #1 and motor #2 VIV-TPSC at: - (*bleu dashed line*) full load;- (*red solid line*) half load;- (*black point line*) without load.

Broken rotor bar fault

The induction motor is directly connected to rated three phase voltage source while one bar in the rotor has been damaged. Figure 4.b shows a drilling hole being performed to obtain one broken rotor bar compared to the healthy one figure 4.a. Different runs with loads conditions (no-load, 50% and full load) have been carried out, the three phase stator currents are measured and the VIV-TPSC is calculated and compared to the CI without fault. Figure 5 shows clearly that broken bar instantaneous variance mean is greater than that of the healthy case irrespective of the load level conditions. The New stator current harmonics with frequencies given by $f_b = (1 \pm k.s) f$ are created in the stator due to broken rotor bar. By sampling the new signals of the currents, the presence of these harmonics will contribute in the calculation of the VIV-TPSC by increasing its value. The advantage of the method lies in the fact that even though the amplitude of these harmonics is very small at no-load (the slip can never actually be null due to the friction) but their small values will certainly affect the mean value and consequently the value of the variance. For more than one broken rotor bar, greater values of the variance of instantaneous variance is expected to be obtained owing to the presence of more harmonics in the measured stator currents.

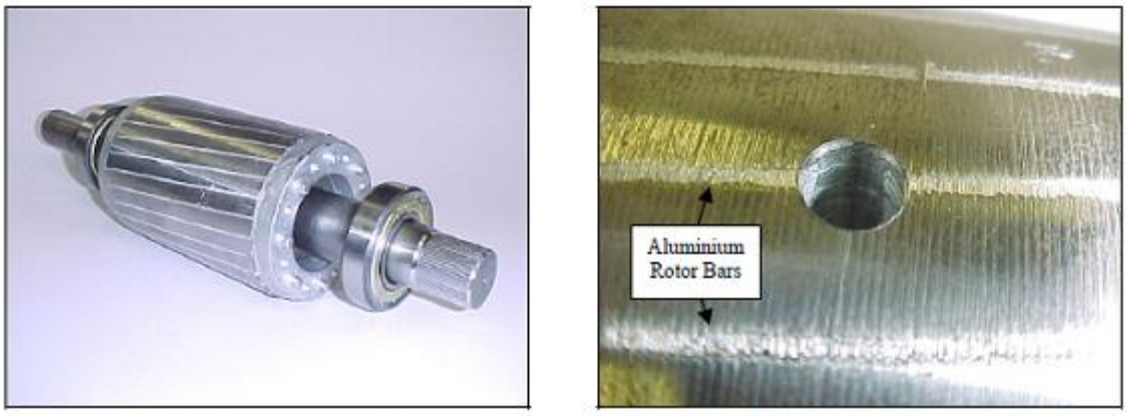

a) Healthy squirrel cage

b) One broken bar squirrel cage

Figure 4: Healthy and one broken bar rotor

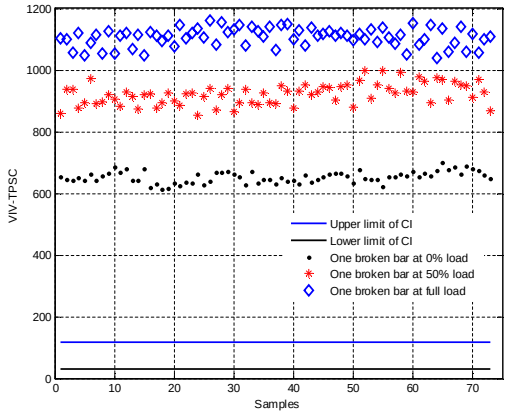

Figure 5: VIV-TPSC of motor #1 with one broken bar fault at different load conditions

Unbalanced supply voltages

The voltage unbalance is introduced while the motor is operating for different load conditions; no-load, 50% and full load. Two tests with respectively 2.5% and 5% of stator voltage unbalance are carried out and the VIV-TPSC is calculated. Figure 6 shows the upper and lower limits of the VIV-TPSC corresponding to the healthy operation of the motor #2 and different faulty VIV-TPSCs due to 2.5% voltage unbalance. It can be easily seen that the VIV-TPSC at different aforementioned loads is outside the 95% confidence tube. Consequently, the faulty VIV-TPSC is still greater than the upper limit of CI independently of the load conditions.

The results shown in figure 7 correspond to the case of 5% voltage unbalance supply. The obtained faulty VIV-TPSC shows clearly in comparison to confidence interval of the healthy case that it is robust against the load variations.

By analysing the stator current owing to voltage unbalance, one can find mainly the 3rd harmonic which is dominant in the spectrum analysis of the current. Although the magnitude is much greater than that of the fundamental, the VIV value is still comparable to that of broken rotor bar motor currents but indeed different.

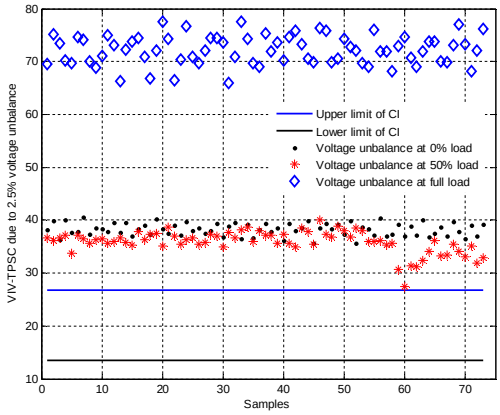

Figure 6: VIV-TPSC of motor #2 with 2.5% voltage unbalance fault at different load conditions

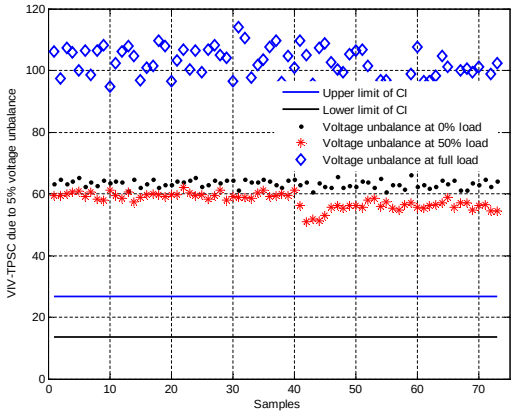

Figure 7: VIV-TPSC of motor #2 with 5% voltage unbalance fault at different load conditions

5. CONCLUSION

In this work a new approach based on the computation of the variance of three-phase stator currents' instantaneous variance (VIV-TPSC) in detecting IM faults at different loads with satisfactory accuracy is proposed. The accuracy, simplicity and efficiency of the algorithm are achieved thanks to an adequately defined confidence interval, hence overcoming the difficulties of parametric uncertainties quantification and devices measurement inaccuracies which increase the number of false alarms. The presented experimental results confirm the capability of the fault detection index based on VIV-TPSC to detect broken rotor bars and voltage unbalance faults. The one broken bar fault, that is difficult to detect by most of the applied detection methods so far, has been detected by the VIV-TPSC algorithm. Besides its simplicity, the proposed algorithm needs only the value of the stator currents making it very suitable for motors monitoring.

References

[1] Sang Bin Lee *et al.*, A New Strategy for Condition Monitoring of Adjustable Speed Induction Machine Drive Systems, IEEE Trans. on Power Electronics, Vol. 26, No. 2, February 2011, pp.389-398.
[2] J. R. Cameron, W. T. Thomson, and A. B. Dow, "Vibration and current monitoring for detecting air-gap eccentricity in large induction motors," Proc. Inst. Elect. Eng., vol. 133, pt. B, pp. 155–163, May 1986.
[3] G. B. Kliman and J. Stein, "Induction motor fault detection via passive current monitoring," in Proc. 1990 Int. Conf. Electrical Machines, vol. 1, Cambridge, MA, pp. 13–17.
[4] G. B. Kliman and J. Stein,, "Methods of motor current signature analysis," Elec. Mach. Power Syst., vol. 20, pp. 463–474, Sept. 1992.
[5] R. R. Schoen, B. K. Lin, T. G. Habetler, J. H. Schlag, and S. Farag,"An unsupervised, on-line system for induction motor fault detection using stator current monitoring," IEEE Trans. Ind. Applicat., vol. 31, pp. 1280–1286, Nov./Dec. 1995.
[6] R. R. Schoen, T. G. Habetler, F. Kamran, and R. G. Bartheld, "Motor bearing damage detection using stator current monitoring," IEEE Trans.Ind. Applicat., vol. 31, pp. 1274–1279, Nov./Dec. 1995.
[7] T. W. S. Chow and G. Fei, "Three phase induction machines asymmetrical faults identification using bispectrum," IEEE Trans. Energy Conversion, vol. 10, pp. 688–693, Dec. 1995.
[8] F. Filippetti, G. Franceschini, C. Tassoni, and P. Vas, "A fuzzy logic approach to on-line induction motor diagnostics based on stator current monitoring," in Proc. 1995 IEEE Int. Power Tech. Conf., vol. EMD, Stockholm, Sweden, pp. 156–161.
[9] M. E. H. Benbouzid and G. Kliman. "Induction Motors' Faults Detection and Localization Using Stator Current Advanced Signal Processing Techniques", IEEE Trans. on Power Electronics, Vol. 14, No. 1, , pp. 14-22, January 1999
[10] W.T. Thomson and M. Fenger. "Current signature analysis to detect induction motor faults". IEEE Industry Applications Magazine. Vol. 7, Issue 4, pp. 26-34. July/August, 2001.
[11] M. O. Mustafa, G. Nikolakopoulos and T. Gustafsson. "Broken bars fault diagnosis based on uncertainty bounds violation for three-phase induction motors", Int. Trans. Electr. Energ. Syst., DOI: 10.1002/etep.1843, 2013
[12] Eduardo Cabal-Yepez, Arturo A. Fernandez-Jaramillo, Arturo Garcia-Perez, Rene J. Romero-Troncoso and Jose M. Lozano-Garcia. "Real-time condition monitoring on VSD-fed induction motors through statistical analysis and synchronous speed observation", Int. Trans. Electr. Energ. Syst., 25, pp. 1657–1672, 2015

[13] P. Naderi and F. Fallahi. “Eccentricity fault diagnosis in three-phase-wound-rotor induction machine using numerical discrete modeling method”, Int. J. Numer. Model. DOI: 10.1002/jnm.2157, 2016
[14] H. Nakamura, S. E. Pandarakone and Y. Mizuno. “A Novel Approach for Detecting Broken Rotor Bar Around Rated Rotating Speed Using Frequency Component and Clustering”, IEEJ Trans., 11(S2), pp. 116–122, 2016
[15] Khaled Yahia, Antonio J. Marques Cardoso, Adel Ghoggal, and Salah-Eddine Zouzou, Induction Motors Broken Rotor Bars Diagnosis Through the Discrete Wavelet Transform of the Instantaneous Reactive Power Signal under Time-varying Load Conditions, Electric Power Components and Systems, 42(7):682–692, 2014
[16] J. R. Millan-Almaraz, R. J. Romero-Troncoso, R. A. Osornio-Rios, and A. Garcia-Perez, Wavelet-based Methodology for Broken Bar Detection in Induction Motors with Variable-speed Drive, Electric Power Components and Systems, 39:271–287, 2011.
[17] S. H. Kia, H. Henao, G.A. Capolino, “Diagnosis of broken-bar fault in induction machines using discrete wavelet transform without slip estimation”, IEEE Trans. Ind. Appl., vol. 45, no. 4, pp. 1395-1404, 2009.
[18] A. Bouzida, O. Touhami, R. Ibtiouen, A. Belouchrani, M. Fadel and A. Rezzoug, “Fault Diagnosis in Industrial Induction Machines through Discrete Wavelet Transform,” IEEE Trans Ind Electron, vol. 58, no. 9, pp. 4385 – 4395, 2011.
[19] A. Sadeghian, Ye. Zhongming and W. Bin, “Online Detection of Broken Rotor Bars in Induction Motors by Wavelet Packet Decomposition and Artificial Neural Networks,” IEEE Trans On Instrum and Measu, vol. 58, no. 7, pp 2253–2263, 2009.
[20] M. A. S. K. Khan, T. S. Radwan, and M. A. Rahman, ‘‘Real-time implementation of wavelet packet transform-based diagnosis and protection of three-phase induction motors,’’ IEEE Trans. Energy *Convers.*, vol. 22, no. 3, pp. 647--655, 2007.
[21] Emin Germen, Murat Başarann, Mehmet Fidan, “Sound based induction motor fault diagnosis using Kohonen self-organizing map”, Mechanical Systems and Signal Processing, 46 (2014) 45–58.
[22] M. E. H. Benbouzid “A review of induction motors signature analysis as a medium for faults detection”, IEEE Trans. on Industrial Electronics, Vol. 14, No. 1, pp. 984-993, October 2000.
[23] H. A. Toliyat and T. A. Lipo, “Transient analysis of cage induction machines under stator, rotor bar and end ring faults,” IEEE Trans. Energy Convers., vol. 10, no. 2, pp. 241–247, Jun. 1995.
[24] S. Williamson and P. Mirzoian, “Analysis of cage induction motor with stator winding faults,” IEEE Trans. Energy Convers., vol. 10, no. 2, pp. 241–247, Jun. 1995.
[25] J. L. Kohler, J. Sottile, and F. C. Trutt, “Alternatives for assessing the electrical integrity of induction motors,” IEEE Trans. Ind. Appl., vol. 28, no. 5, pp. 1109–1117, Sep./Oct. 1992.
[26] M. Arkan, D. K. Perovic, and P. Unsworth, “Online stator fault diagnosis in induction motors,” Proc. Inst. Elect. Eng., Elect. Power Appl., vol. 148, no. 6, pp. 537–547, Nov. 2001.
[27] Pu Shin, Zheng Chen, Yuriy Vagapov, Zoubir Zouaoui, A new diagnosis of broken rotor bar fault extent in three phase squirrel cage induction motor, Mechanical Systems and Signal Processing 42 (2014) 388–403.
[28] Hernandez-Vargas, M., Cabal-Tepez, E., Garcia-Perez, A., “A new diagnosis of broken rotor bar fault extent in three phase squirrel cage induction motor”, Comput Electr Eng (2014), http://dx.doi.org/10.1016/j.compeleceng.2013.12.020.
[29] W. J. Conover, Practical non-parametric statistics, Wiley Series in Probability and Statistics, 3rd edition, 1999.